The Plant Cell, Vol. 15, 465–480, February 2003, www.plantcell.org © 2003 American Society of Plant Biologists

Plant γ-Tubulin Interacts with αβ-Tubulin Dimers and Forms Membrane-Associated Complexes

Denisa Dryková,[a,1] Věra Cenklová,[b,1] Vadym Sulimenko,[c] Jindřich Volc,[a] Pavel Dráber,[c] and Pavla Binarová[a,2]

[a] Institute of Microbiology, Academy of Sciences of the Czech Republic, Vídeňská 1083, 142 20 Prague 4, Czech Republic
[b] Institute of Experimental Botany, Academy of Sciences of the Czech Republic, Sokolovská 6, 772 00 Olomouc, Czech Republic
[c] Institute of Molecular Genetics, Academy of Sciences of the Czech Republic, Vídeňská 1083, 142 20 Prague 4, Czech Republic

γ-Tubulin is assumed to participate in microtubule nucleation in acentrosomal plant cells, but the underlying molecular mechanisms are still unknown. Here, we show that γ-tubulin is present in protein complexes of various sizes and different subcellular locations in Arabidopsis and fava bean. Immunoprecipitation experiments revealed an association of γ-tubulin with αβ-tubulin dimers. γ-Tubulin cosedimented with microtubules polymerized in vitro and localized along their whole length. Large γ-tubulin complexes resistant to salt treatment were found to be associated with a high-speed microsomal fraction. Blue native electrophoresis of detergent-solubilized microsomes showed that the molecular mass of the complexes was >1 MD. Large γ-tubulin complexes were active in microtubule nucleation, but nucleation activity was not observed for the smaller complexes. Punctate γ-tubulin staining was associated with microtubule arrays, accumulated with short kinetochore microtubules interacting in polar regions with membranes, and localized in the vicinity of nuclei and in the area of cell plate formation. Our results indicate that the association of γ-tubulin complexes with dynamic membranes might ensure the flexibility of noncentrosomal microtubule nucleation. Moreover, the presence of other molecular forms of γ-tubulin suggests additional roles for this protein species in microtubule organization.

INTRODUCTION

The successive replacement of microtubular arrays (cortical microtubules, preprophase band, mitotic spindle, and phragmoplast) during cell cycle progression is unique to higher plants. This flexibility in building microtubule structures at different locations can be achieved in plants because the dominating microtubule organizing centers, which are comparable to those of animal centrosomes, are missing in both somatic and gametic cells. However, centrosomes are not absolutely required for microtubule nucleation even in animal cells. It was shown that microtubules could be nucleated in the absence of centrosomes, presumably by yet undefined cytoplasmic factors (Vorobjev et al., 1997). For an understanding of how microtubules are nucleated and organized without the centrosome, the first step is to identify the molecular composition of the dispersed microtubule nucleation sites.

γ-Tubulin is a highly conserved member of the tubulin superfamily that is located on the minus end of microtubules in microtubule organizing centers, where such structures are present in the cell (Wiese and Zheng, 1999). Although in animal cells, γ-tubulin participates in the nucleation of microtubules from microtubule organizing centers, the majority of this protein is associated with other centrosomal proteins in soluble cytoplasmic complexes. Large (~2.2 MD) γ-tubulin ring complexes (γ-TuRCs) and smaller (~280 kD) γ-tubulin complexes were identified in various species (Moritz et al., 1995; Zheng et al., 1998; Oegema et al., 1999). γ-Tubulin complexes comprise two molecules of γ-tubulin and one molecule each of GCP2 and GCP3 (γ-tubulin complex proteins), which are homologs of the *Saccharomyces cerevisiae* proteins Spc97p and Spc98p (Geissler et al., 1996). The γ-TuRCs are formed by small complexes and by other proteins. In addition to nucleation from the microtubule organizing center, the large complexes also are involved in regulating the dynamics of the microtubule minus ends (Wiese and Zheng, 2000). Recently, genetic data from *Schizosaccharomyces pombe* and *Aspergillus nidulans* showed that γ-tubulin might play other important roles in the organization of mitotic and cytokinetic microtubules (Hendrickson et al., 2001; Jung et al., 2001).

[1] These authors contributed equally to this article.
[2] To whom correspondence should be addressed. E-mail binarova@biomed.cas.cz; fax 420-2-41062384.
Article, publication date, and citation information can be found at www.plantcell.org/cgi/doi/10.1105/tpc.007005.

In plants, γ-tubulin was immunolocalized preferentially on microtubules (Liu et al., 1993). The association of γ-tubulin with kinetochore microtubules and the presence of γ-tubulin in premitotic nuclei suggested its role in microtubule and spindle organization (Binarova et al., 1998, 2000; Petitpren et al., 2001). Immunolocalization studies with different antibodies reported a punctuated labeling for γ-tubulin with nuclear and cortical membranes and with organelle-like structures (McDonald et al., 1993; Liu et al., 1994; Dibbayawan et al., 2001). Soluble cytoplasmic γ-tubulin complexes were identified in fava bean and maize cell extracts (Binarova et al., 2000; Stoppin-Mellet et al., 2000). The latter authors reported a γ-tubulin association with the microsomal fraction. Despite many data suggesting that γ-tubulin is an abundant protein at various locations in acentrosomal plant cells, its role in plant microtubule nucleation and organization is still largely unknown.

Here, we show that plant γ-tubulin is present in the form of protein complexes of various sizes and of different properties. Soluble γ-tubulin interacts with tubulin dimers and cosediments with microtubules in vitro. We report that large γ-tubulin complexes active in microtubule nucleation are associated with membranes. This association of γ-tubulin with membranous structures might ensure the nucleation of microtubule arrays from dispersed sites in acentrosomal cells.

RESULTS

Anti-Peptide Antibodies Raised against Different Parts of the γ-Tubulin Molecule Recognize γ-Tubulins in Several Plant Species

As a prerequisite to the study of γ-tubulin in higher plant cells, plant-specific polyclonal antibody (AthTU) was raised against a 14–amino acid peptide (EYKACESPDYIKWG) corresponding to the Arabidopsis γ-tubulin sequence 437 to 450. Affinity-purified antibody recognized a single band of 56 kD in Arabidopsis and a slightly larger (by ~1 to 2 kD) band in maize, fava bean, and pea (Figures 1A and 1B, AthTU). A similar staining pattern was seen with a polyclonal antibody raised against the human γ-tubulin sequence 38 to 50, but the antibody reactivity was substantially weaker (data not shown). Monoclonal antibody TU-31 raised against a peptide corresponding to the human γ-tubulin sequence 434 to 449 gave similar immunoblot staining in all of the species tested. One extra band of ~60 kD was detected in Arabidopsis (Figures 1A and 1B, TU-31); higher resolution conditions during electrophoresis revealed two corresponding, very close bands in other plant species (data not shown). The same staining pattern was obtained with extracts from seedlings or cell cultures (Arabidopsis) or with extracts from root meristems or whole seedlings (in all other species analyzed). Like the pattern shown previously for TU-31 antibody

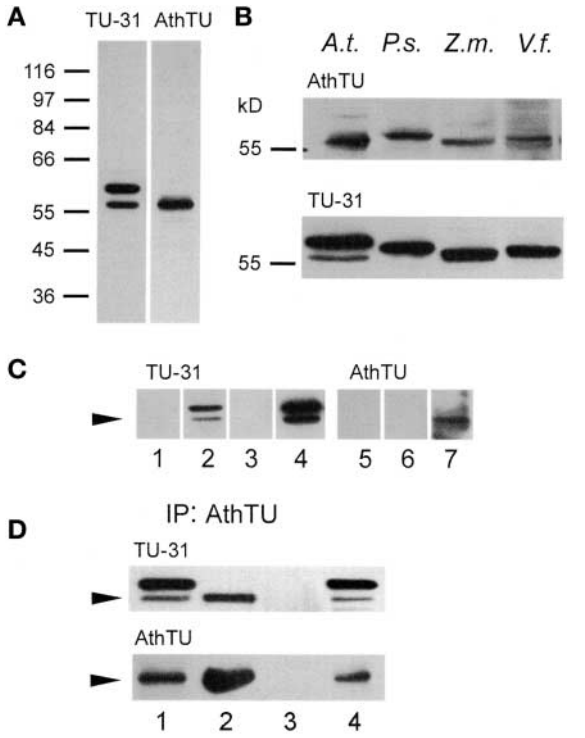

Figure 1. Immunoblot Analysis of Cell Extracts with Polyclonal and Monoclonal Anti-γ-Tubulin Antibodies.

(A) Affinity-purified AthTU antibody recognized one band in Arabidopsis extracts. Two bands were recognized with monoclonal antibody TU-31.

(B) Immunoblot detection of γ-tubulin in several plant species. Cell extracts from Arabidopsis (*A.t.*), pea (*P.s.*), maize (*Z.m.*), and fava bean (*V.f.*) were separated by 10% SDS-PAGE and stained with polyclonal antibody AthTU and monoclonal antibody TU-31.

(C) Immunostaining of γ-tubulin on blots was abolished after preabsorption of antibodies with immunizing peptide. Antibodies TU-31 (lanes 1 to 4) and AthTU (lanes 5 to 7) were preabsorbed with the immunizing peptides and used to probe 10% SDS-PAGE–separated Arabidopsis extracts. Lanes 1 and 6, peptide used to prepare the TU-31 antibody; lanes 2 and 7, no peptide; lanes 3 and 5, peptide used to prepare the AthTU antibody; lane 4; negative control peptide. The arrowhead indicates the position of the 56-kD γ-tubulin.

(D) γ-Tubulin immunoprecipitated (IP) with AthTU antibody was immunodetected with both TU-31 and AthTU antibodies. Lane 1, extract before immunoprecipitation; lane 2, immunoprecipitated and peptide-eluted γ-tubulin; lane 3, control eluate from beads with preimmune serum; lane 4, supernatant after immunoprecipitation. Both antibodies recognized immunopurified γ-tubulin (56 kD). Arrowheads indicate the position of the 56-kD γ-tubulin.

(Binarova et al., 2000), the AthTU antibody recognized γ-tubulin in nuclear extracts (data not shown).

Preabsorption of TU-31 with the peptide used for immunization (Figure 1C, lane 1) or with the Arabidopsis-specific homologous peptide used for the preparation of AthTU anti-

body (Figure 1C, lane 3) prevented the staining of both bands on blots from extracts of Arabidopsis. Both peptides also prevented immunolabeling with AthTU antibody (Figure 1C, lanes 5 and 6). On the other hand, immunolabeling was not influenced by the preabsorption of TU-31 with human γ-tubulin peptide from the N-terminal region of the molecule (Figure 1C, lane 4).

Immunoprecipitation of γ-tubulin from Arabidopsis extracts with AthTU antibody followed by specific elution with corresponding immunizing peptide revealed that the immunoprecipitated 56-kD protein is recognized by both antibodies (Figure 1D, TU-31 [lane 2] and AthTU [lane 2]). When immunoglobulins isolated from preimmune serum were used for precipitation instead of AthTU antibody, no γ-tubulin was eluted with the immunizing peptide (Figure 1D, lane 3). These data demonstrate that both the plant γ-tubulin–specific polyclonal antibody AthTU and the monoclonal antibody TU-31 can be used as markers for γ-tubulin.

Immunofluorescence Analysis Indicates an Association of γ-Tubulin with Microtubules and Membranes

The immunofluorescence staining pattern obtained with affinity-purified AthTU antibody was similar to that described previously for the monoclonal anti-γ-tubulin antibody TU-32 (Binarova et al., 1998, 2000). Punctate γ-tubulin staining was associated with microtubule arrays, localized in the vicinity of nuclei and the cell cortex and in the area of cell plate formation, and provided cell cycle–dependent nuclear staining. Double-label staining of cells with AthTU and anti-α-tubulin antibody showed an association of γ-tubulin with kinetochore microtubules and an accumulation of signal on poles on which acentrosomal spindle is seemingly anchored to the plasma membrane and/or the membranes of polar vacuoles (Figure 2A). To characterize the interaction of γ-tubulin with membranes, antibodies visualizing the *trans*-Golgi network and/or the nuclear membrane were used in double-labeling experiments with anti-γ-tubulin antibodies. Spindle-associated γ-tubulin was on the poles localized close to the Golgi membranes in metaphase (Figure 2B) as well as in anaphase (Figure 2C), when the majority of γ-tubulin accumulated, with the shortening kinetochore fibers focused on the poles. When chromosomes reached the poles, an intensive granular signal of γ-tubulin was associated with remnants of kinetochore microtubules (Figure 2D, arrow). These γ-tubulin–decorated polar structures were localized in the vicinity of the Golgi membranes (Figure 2E, arrow). The inhibitory effect of brefeldin A on Golgi trafficking in plant cells was characterized (Ritzenthaler et al., 2002). Using this pharmacological approach, we observed that 30 min of treatment of fava bean roots with 200 $\mu g \cdot ml^{-1}$ brefeldin A induced the formation of multipolar spindles, with γ-tubulin accumulated with aberrantly located spindle poles (Figure 2F).

γ-Tubulin remained in the kinetochore area oriented to the cell cortex (Figure 2D, arrow) even after kinetochore microtubules disappeared and the anaphase spindle was rearranged into the early phragmoplast. The majority of γ-tubulin in telophase was present in the phragmoplast area, but punctate labeling also was localized around the newly formed nuclear envelope. Double labeling of cells with anti-γ-tubulin antibody and with antibody staining the nuclear envelope marker importin revealed that γ-tubulin is not colocalized with importin on the nuclear envelope but is present in spots mainly in the polar region in the vicinity of the nuclei (Figure 2H).

γ-Tubulin Is Present in the Cytosolic Fraction in the Form of Protein Complexes

In our previous experiments, we determined that γ-tubulin is present in plant extracts in the form of protein complexes (Binarova et al., 2000); here, we analyzed the size distribution of γ-tubulin in cell extracts of fava bean and Arabidopsis using gel filtration chromatography and nondenaturing electrophoresis. After gel filtration, γ-tubulin was distributed in a wide zone, but the first narrow maximum was in fractions 2 to 5, close to the column void volume (~2 MD). This result suggested that γ-tubulin is part of a large complex in Arabidopsis (Figure 3A) as well as in fava bean (Figure 3C). Intermediate-sized γ-tubulin complexes, ranging from ~400 to 900 kD, and smaller complexes than these also were found in extracts from both species. Because it is known from animal cell model systems that the large γ-tubulin complexes disassemble to smaller complexes in the presence of 500 mM NaCl (Oegema et al., 1999), the same separation conditions were used. As shown in Figure 3B, there was no reduction in the amount of γ-tubulin incorporated into large complexes. On the other hand, salt treatment reduced the amount of some types of γ-tubulin intermediate complexes (Figure 3B).

The size and abundance of the intermediate complexes varied among individual experiments, suggesting their dynamics. High-salt treatment also abolished the immunolabeling for γ-tubulin in fractions corresponding in molecular mass to monomers or smaller fractions, resulting from the apparent retention of γ-tubulin in the gel matrix. Similar profiles of γ-tubulin (56 kD) were found in Arabidopsis stained with the polyclonal antibody AthTU and the monoclonal antibody TU-31. However, antibody TU-31 also stained a 60-kD band distributed in fractions corresponding to 120 to 240 kD (Figure 3B, TU-31). αβ-Tubulin dimers were coeluted with γ-tubulin in a broad zone of fractions, with a large molecular mass maximum of ~2 MD (Figure 3A, α-tubulin and β-tubulin). In contrast to γ-tubulin, in which intermediate-sized complexes diminish in the presence of high salt concentrations, intermediate protein complexes containing αβ-tubulin dimers were more stable (Figure 3B).

The presence of γ-tubulin complexes of various sizes also was confirmed by electrophoretic separation of fractions

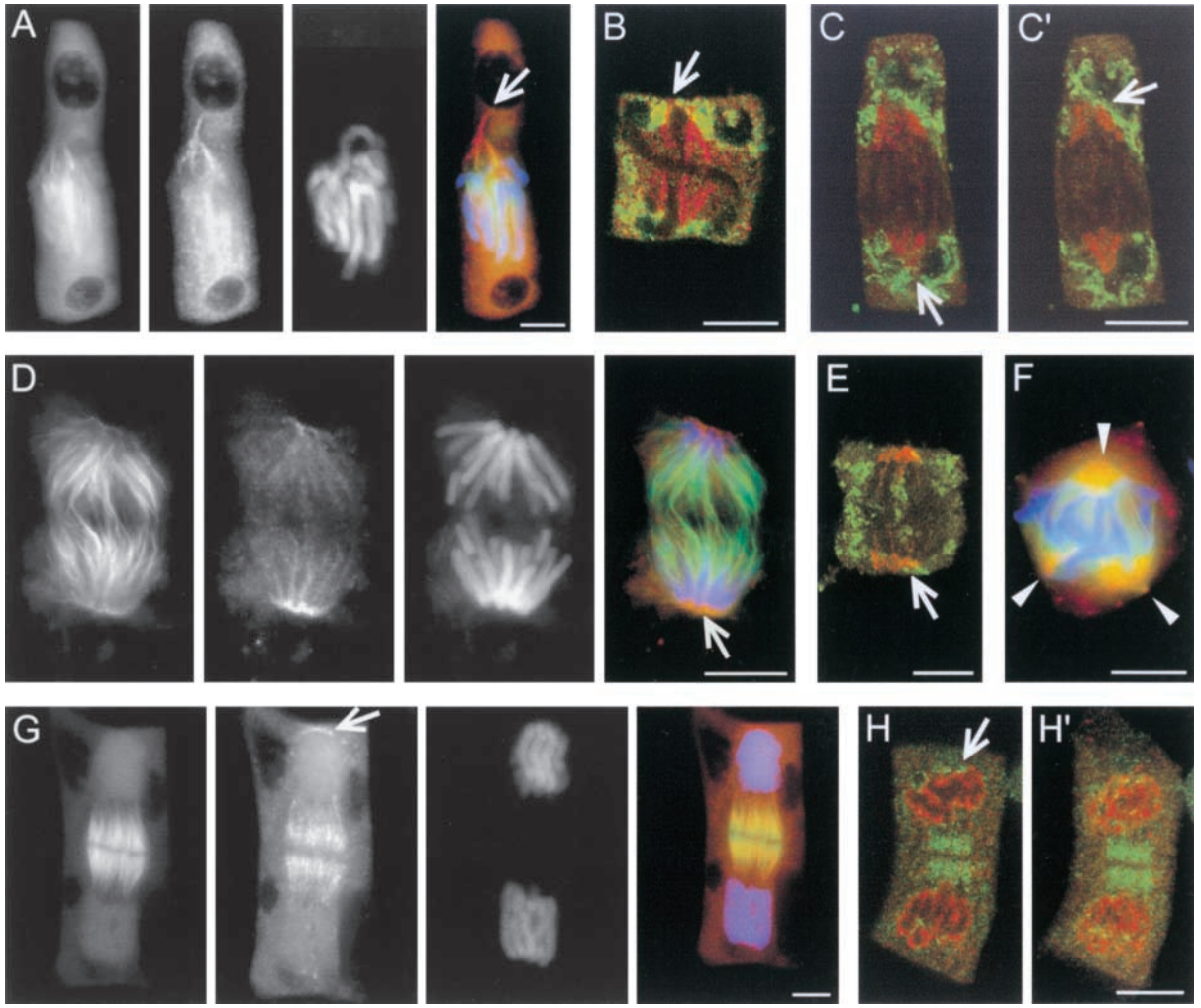

Figure 2. Subcellular Localization of γ-Tubulin in Mitotic Cells.

Root meristem cells of fava bean were stained with rabbit affinity-purified anti-γ-tubulin antibody AthTU (red), mouse monoclonal anti-α-tubulin antibody DMA1 (green), and 4′,6-diamidino-2-phenylindole (blue) for chromatin visualization.

(A), **(D)**, **(F)**, and **(G)** γ-Tubulin was visualized with anti-rabbit Cy3-conjugated antibody, and DMA1 antibody was visualized with anti-mouse fluorescein isothiocyanate (FITC)–conjugated antibody. Golgi membranes in root meristem cells of fava bean were stained with polyclonal rabbit TLG antibody (green) and visualized with anti-rabbit FITC-conjugated antibody.

(B), **(C)**, and **(E)** γ-Tubulin was stained with mouse monoclonal TU-31 antibody (red) and visualized with anti-mouse Cy3-conjugated secondary antibody.

(H) The nuclear envelope marker importin was stained with monoclonal mouse antibody (red) and visualized with anti-mouse Cy3-conjugated antibody. γ-Tubulin was stained with rabbit polyclonal antibody AthTU (green) and visualized with anti-rabbit FITC-conjugated secondary antibody.

(A) Metaphase cell with γ-tubulin anchoring kinetochore spindle microtubules to the vacuolar membrane (arrow).

(B) Confocal laser scanning microscopy (CLSM) single optical section of a metaphase cell with γ-tubulin localized with the metaphase spindle and the Golgi membranes in the area of the spindle poles (arrow).

(C) and **(C′)** Two CLSM optical sections of an anaphase cell with γ-tubulin associated with shortening kinetochore fibers and with the Golgi membranes in the vicinity of the spindle poles (arrows).

(D) A cell later in anaphase shows accumulation of γ-tubulin in the kinetochore region on the spindle poles (arrow).

(E) CLSM single optical sections of a cell in the same stage of mitosis as in **(D)** shows that γ-tubulin–decorated structures in the kinetochore region on poles are associated with the Golgi membranes (arrow).

(F) Multipolar mitosis observed after 30 min of brefeldin A treatment (arrowheads indicate multiple poles with γ-tubulin).

(G) Late anaphase/early telophase cell with remnants of γ-tubulin associated with kinetochores (arrow), whereas kinetochore microtubules had already disappeared.

(H) and **(H′)** CLSM single optical sections **(H)** and reconstitution of image stacks **(H′)** of telophase cells demonstrating that importin decorates the newly formed nuclear envelope and that γ-tubulin labeling is present mainly in the phragmoplast area and in spots in the vicinity of the nuclei.

(A), **(D)**, **(F)**, and **(G)** are images from classic immunofluorescence microscopy. **(B)**, **(C)**, **(E)**, and **(H)** are images from CLSM. Bars = 10 μm.

from gel filtration of Arabidopsis extracts under nondenaturing conditions. Staining of blots with antibody AthTU showed that γ-tubulin is present in both large complexes (gel filtration fractions 3 to 7) and smaller complexes (fractions 15 to 23). In the latter case, γ-tubulin staining appeared in fuzzy broad bands with relative molecular masses corresponding approximately to the sizes of the large and smaller complexes estimated by gel filtration (Figure 4A). The results shown are for the gel filtration performed in the presence of 500 mM NaCl, which should reduce the nonspecific interactions of γ-tubulin with other proteins or γ-tubulin aggregation during sample preparation. To exclude the possibility that broad diffuse bands resulted from the presence of 500 mM NaCl, samples were transferred before electrophoresis to the buffer with 50 mM salt. Fuzzy bands were present; moreover, reconstitution of intermediate-sized complexes was observed (data not shown). The fuzzy bands probably reflect the heterogeneity of γ-tubulin complexes or γ-tubulin oligomers, because other cytoplasmic proteins migrated under the same conditions as distinct bands.

The monoclonal antibody TU-31, like the AthTU antibody, recognized γ-tubulin in large complexes (Figure 4B). Intense staining of bands in the region 120 to 220 kD probably reflects the presence of complexes containing a 60-kD protein recognized by the TU-31 antibody (Figure 3B, TU-31). Therefore, both antibodies provide similar staining in high molecular mass fractions, but they clearly differ in staining in lower molecular mass fractions. Collectively, these data indicate that in cytosolic fractions there are tubulin protein complexes of different properties.

γ-Tubulin Is Associated with Membrane Microsomal Fractions

To analyze the interaction of plant γ-tubulin with membranes (as indicated by immunofluorescence analysis), total cell extracts of fava bean and Arabidopsis were separated by differential centrifugation into cytosolic and membrane fractions. The data obtained for fava bean and Arabidopsis were very similar; therefore, only Arabidopsis data are presented. In Figure 5A, the relative distribution of γ-tubulin in

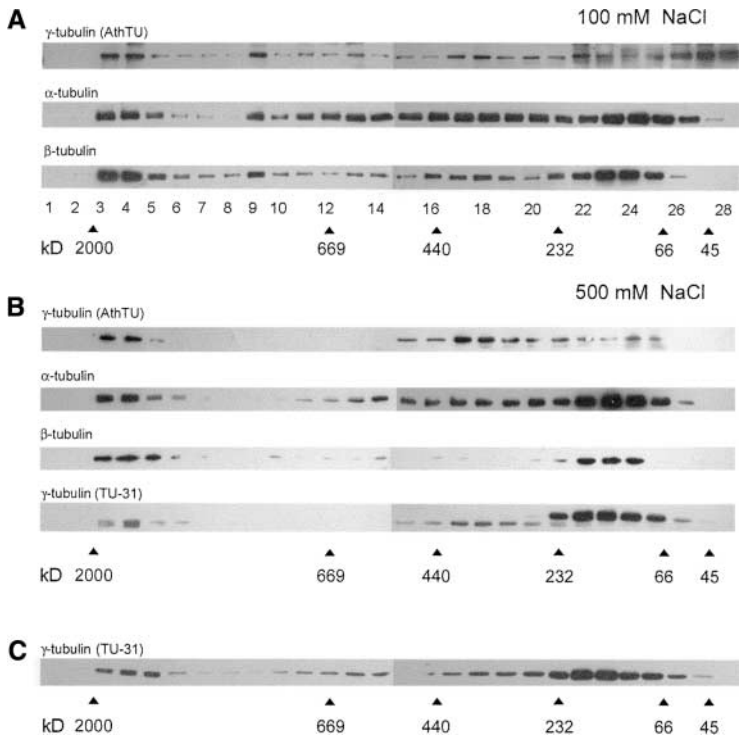

Figure 3. Gel Filtration of Cytoplasmic Extracts Followed by SDS-PAGE Analysis.

(A) and **(B)** Fractionations from gel filtration of Arabidopsis extracts in the presence of 100 **(A)** or 500 **(B)** mM NaCl.
(C) Fractionations from gel filtration of fava bean extract.
Fractions were analyzed by 10% SDS-PAGE, immunoblotted with antibodies AthTU and TU-31 against γ-tubulin and DM1A against α-tubulin, and reblotted with TUB 2.1 antibody against β-tubulin. Calibration standards (in kD) are indicated with arrowheads. Numbers from 1 to 28 denote individual fractions.

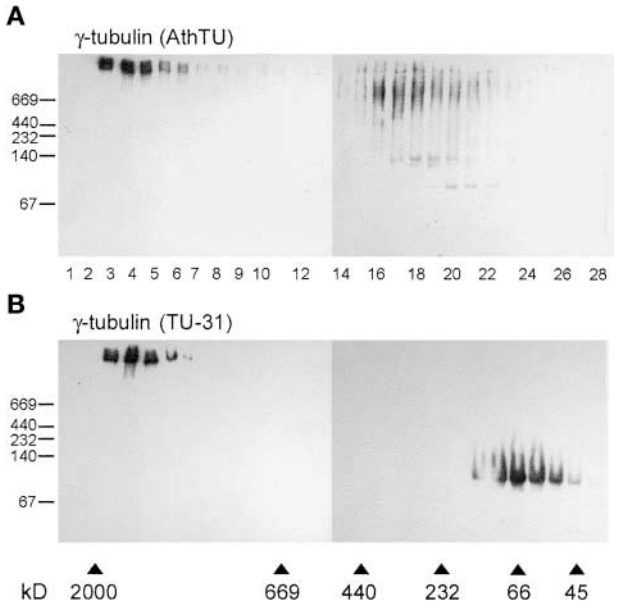

Figure 4. Gel Filtration of Cytoplasmic Extracts Followed by Nondenaturing PAGE Analysis.

Arabidopsis extracts were subjected to gel filtration chromatography in the presence of 500 mM NaCl. Fractions were analyzed by 3 to 10% native PAGE and immunoblotted with antibodies AthTU **(A)** and TU-31 **(B)** against γ-tubulin. Molecular mass standards (in kD) are indicated with arrowheads. Numbers from 1 to 28 denote individual fractions.

cytosolic and membrane fractions is shown; in Figure 5B, the same amount of protein was loaded from each fraction. After low-speed centrifugation, γ-tubulin was present in the pellet (P4) as well as in the supernatant (S4). After further spinning (27,000*g* for 60 min) of the supernatant (S4), a smaller amount of γ-tubulin was detected in the pellet (P27) containing mainly mitochondria, plastids, and larger microsomes. The majority of γ-tubulin remained in the supernatant (S27), from which a high-speed microsomal pellet (P100) was obtained by further centrifugation (100,000*g* for 60 min). P100 contained small vesicles with diameters of ~100 to 300 nm. The composition of P27 and P100 was checked by electron microscopy (data not shown).

As shown in Figure 5A, ~50% of γ-tubulin from supernatant S27 was spun down to pellet P100. γ-Tubulin was solubilized almost completely from P100 by the detergent 3-[(3-cholamidopropyl)dimethylammonio]-1-propanesulfonic acid (CHAPS) (Figures 5A and 5B, P100 S_{CH} for solubilized membrane proteins and P100 P_{CH} for insoluble membrane material). The detergents CHAPS and β-D-lauryl maltoside solubilized almost all γ-tubulin from the microsomal pellet (P100), whereas other detergents (0.1% Triton X-100 or 0.1% Nonidet P-40) were less effective. Treatment of the pellet (P100) with Na_2CO_3, pH 11, used to strip extrinsic or absorbed proteins, was much less efficient in the solubilization of γ-tubulin than the detergents used (data not shown). With TU-31 antibody, the pattern of fractionation of the 56-kD γ-tubulin was similar to that seen with AthTU antibody. However, the 60-kD protein detected by TU-31 was enriched in high-speed supernatant (S100), and only a very small amount of this protein was found in the microsomal membrane fraction (P100 S_{CH}) (Figure 5B, TU-31). This result indicates a different subcellular localization of the 56-kD γ-tubulin and the 60-kD protein. Homogenization with liquid nitrogen and in cold buffer using a prechilled blender gave the same results, excluding the effect of the homogenization procedure on γ-tubulin distribution.

The distribution of tubulin dimers among fractions was similar to that of γ-tubulin, and α- and β-tubulin were solubilized together with γ-tubulin from the microsomal fraction (Figure 5A). On the other hand, the small GTPase Ran, an abundant cytosolic protein used as a control, was found only in the soluble cytosolic fraction but not in the fraction containing microsomal membranes (Figure 5A, Ran). We conclude that γ-tubulin and αβ-tubulin dimers are associated with plant membranes, mainly in the high-speed microsomal fraction.

Blue Native PAGE Confirms That γ-Tubulin Is Associated with Membranes in the Form of Large Protein Complexes

Nondenaturing blue native PAGE (BN-PAGE) was developed for the isolation of membrane-associated protein complexes (Caliebe et al., 1997). To further examine the association of γ-tubulin with membranes, samples from cell fractionation were subjected to BN-PAGE in the first dimension and SDS-PAGE in the second dimension. Antibody AthTU strongly reacted with material electrophoretically separated from the supernatant (S27) with protein complexes of >1 MD (Figure 6, S27). Intermediate complexes also were detected, and there was no γ-tubulin in the monomeric form. Reprobing of membranes with anti-α-tubulin antibody revealed a large distribution of α-tubulin, with molecular masses corresponding to large complexes and to monomers (Figure 6, S27). A similar distribution was found for β-tubulin (data not shown). Further fractionation of S27 to the high-speed supernatant and pellet showed that smaller γ-tubulin complexes remained in the supernatant (Figure 6, S100). The majority of large γ-tubulin complexes were pulled down to the high-speed microsomal pellet, from which they were solubilized by lauryl maltoside (Figure 6, $P100S_L$). α-Tubulin (Figure 6, $P100S_L$) and β-tubulin (data not shown) also were detected in the large membrane-associated complexes. Similar data were obtained regardless of the differing extraction procedures (frozen cells ground in liquid nitrogen or fresh cells ground with a blender) or detergents (CHAPS or lauryl maltoside) used for solubilization of the membrane protein. These data indicate that stable large

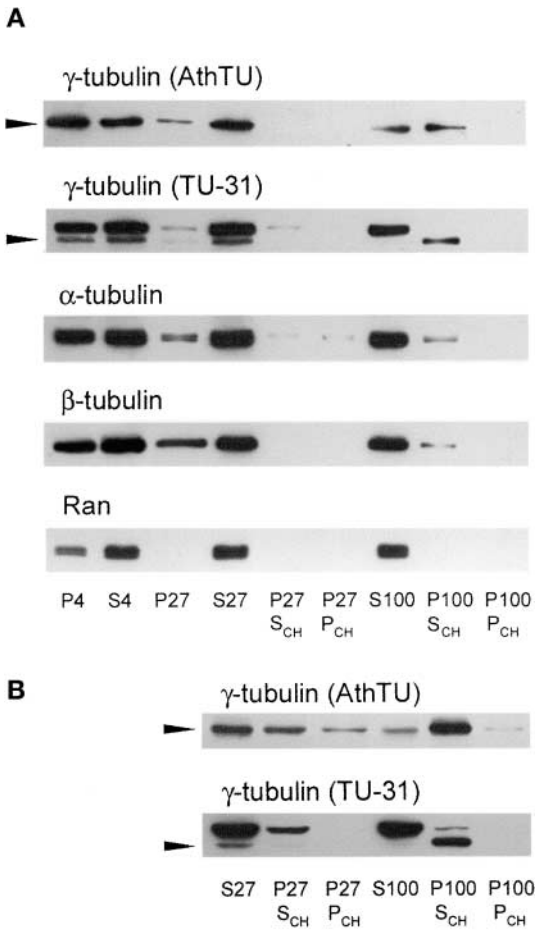

Figure 5. Distribution of γ-Tubulin in Cytoplasmic and Membrane Fractions.

Cell extracts from Arabidopsis were differentially centrifuged, and pellets were extracted with CHAPS.
(A) To compare the relative distribution of immunoblotted proteins, pelleted material was resuspended in a volume equal to the volume of the corresponding supernatant.
(B) Samples loaded at the same protein content (10 μg/lane).
Samples were analyzed by 10% SDS-PAGE and immunoblotted with antibodies AthTU and TU-31 against γ-tubulin, DM1A against α-tubulin, TUB 2.1 against β-tubulin, and anti-Ran antibody. P4 and S4, low-speed pellet and supernatant (4000*g* for 10 min); P27 and S27, pellet and supernatant after centrifugation of the S4 supernatant (27,000*g* for 1 h); P27 S_{CH} and P27 P_{CH}, supernatant and pellet after solubilization of the P27 pellet with CHAPS; S100, high-speed supernatant after centrifugation of the S27 supernatant (100,000*g* for 1 h); P100 S_{CH} and P100 P_{CH}, supernatant and pellet after solubilization of the P100 pellet with CHAPS. Arrowheads indicate the position of the 56-kD γ-tubulin.

γ-tubulin complexes containing tubulin dimers are associated with microsomal membranes.

Large γ-Tubulin Complexes Are Potent Microtubule Nucleators

The functional assay–cover slip nucleation assay (Oegema et al., 1999), developed originally to test the nucleation activity of γ-tubulin complexes in *Drosophila*, was modified and used to determine the microtubule nucleation activity of fractions from gel filtration of the Arabidopsis cell extract. Purified bovine brain tubulin at a concentration of 0.5 mg/mL, which was shown to be subcritical for spontaneous tubulin polymerization, was used in all nucleation assays. The results are shown in Figure 7, in which all of the micrographs were made under the same exposure conditions. Maximal tubulin polymerization was observed with fractions 3 to 4,

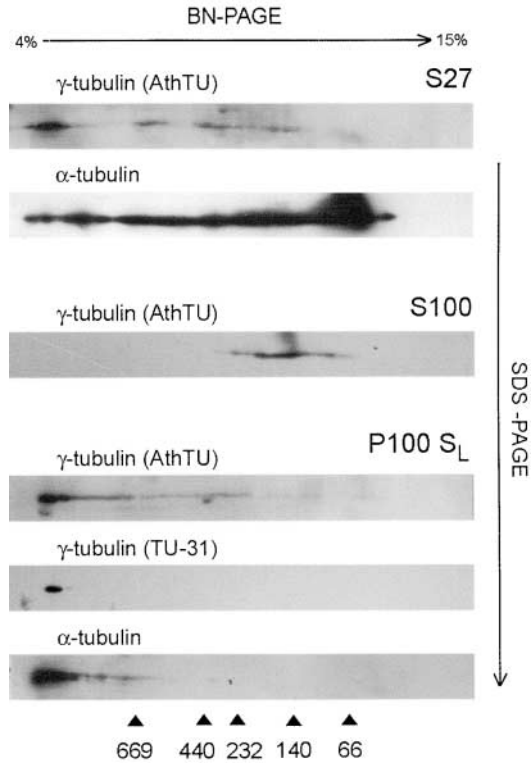

Figure 6. BN-PAGE of Cell Extracts and Solubilized Microsomes.

S27, S100, and lauryl maltoside–solubilized microsomal proteins (P100 S_L), as described in the legend to Figure 5, were separated in the first dimension by 4 to 15% BN-PAGE and in the second dimension by 10% SDS-PAGE. Separated proteins were immunoblotted with antibodies AthTU and TU-31 against γ-tubulin and DM1A against α-tubulin. Molecular mass standards (in kD) for the first dimension are indicated with arrowheads at bottom.

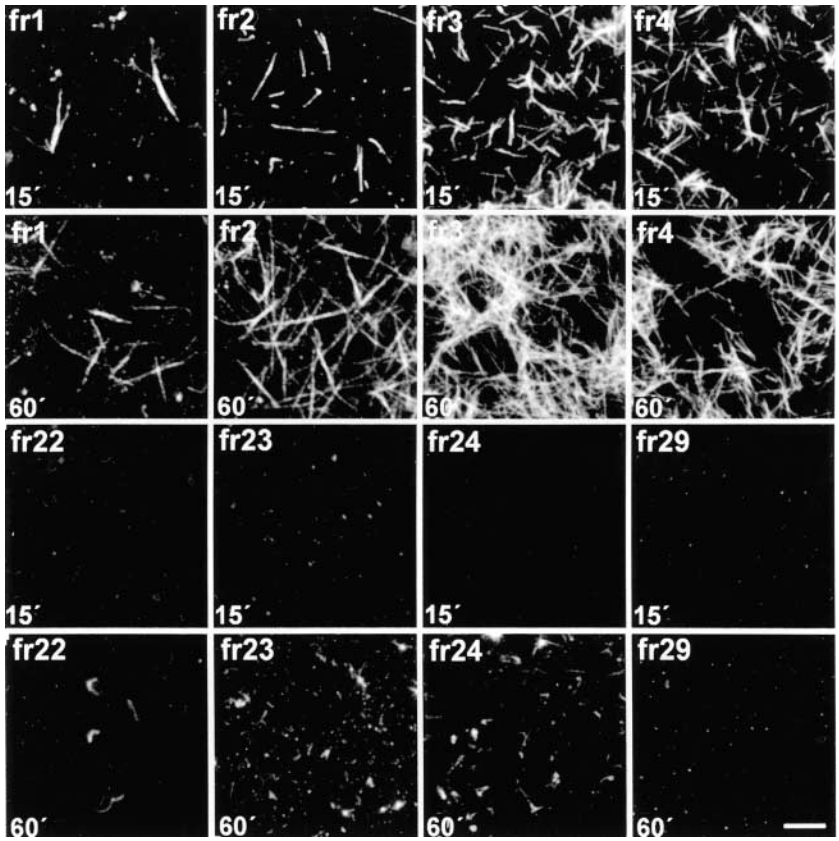

Figure 7. Analysis of Fractions from Gel Filtration Using the Cover Slip Nucleation Assay.

Selected fractions from gel filtration of Arabidopsis (S27) extracts were used for the cover slip microtubule nucleation assay performed as described in Methods. The top two rows represent fractions containing large γ-tubulin complexes (fr1 to fr4) after incubation with brain tubulin for 15 min (15′) or 60 min (60′). The bottom two rows represent fractions containing small γ-tubulin complexes (fr22 to fr24) and a control without γ-tubulin (fr29) after incubation with brain tubulin for 15 min (15′) or 60 min (60′). Microtubules were visualized by immunofluorescence microscopy with anti-α-tubulin antibody DM1A. Equivalent exposures are presented. Bar = 10 μm.

corresponding to the large γ-tubulin complexes. Microtubules were found after 15 min of polymerization, and their number increased after 1 h of polymerization (Figure 7, top two rows). No microtubule polymerization was observed with fractions 22 to 24, which contained γ-tubulin in the form of smaller complexes (Figure 7, bottom two rows), or with fraction 29, in which γ-tubulin was not detected and which served as a negative control. Data from several independent nucleation experiments with gel filtration samples from Arabidopsis and fava bean cell extracts confirmed that the number of microtubules formed in the presence of fractions 2 to 5 correlated with the amount of γ-, α-, and β-tubulins immunodetected in these fractions. Little (or no) nucleation activity was observed when fractions from gel filtration of high-speed supernatants (S100), which were largely depleted in large γ-tubulin complexes, were tested in the assays.

Coprecipitation of γ-Tubulin with αβ-Tubulin Dimers

Because our data showed a codistribution of tubulin dimers with γ-tubulin during fractionation procedures, we tried to determine whether γ-tubulin in the soluble cytoplasmic pool interacts with tubulin dimers. As shown in Figure 1C, immunoprecipitation of γ-tubulin from Arabidopsis extracts with AthTU antibody followed by specific elution with the immunizing peptide revealed that a 56-kD protein was recognized by both TU-31 and AthTU antibodies. γ-Tubulin (56 kD) was precipitated specifically from Arabidopsis extracts with immobilized anti-γ-tubulin antibody TU-31, as demonstrated by the staining of blots with the plant-specific anti-γ-tubulin antibody AthTU (Figure 8A, lane 5). When the immobilized antibody was incubated without extract, no staining in the position of γ-tubulin was observed and no binding of γ-tubulin to immobilized protein L was detected (Figure 8A,

lanes 4 and 6). The control antibody NF-09 gave no precipitation of γ-tubulin (Figure 8A, lane 3). The faint staining in lanes 2 to 5 of Figure 8A represents the heavy chains of immunoglobulins. When the TU-31–precipitated material was probed with mouse antibodies against tubulin subunits, the heavy chains of mouse IgG obscured the detection of coprecipitated tubulin dimers. Therefore, immobilized anti-β-tubulin antibody TU-06 (IgM) was used, which specifically precipitated tubulin dimers, as documented by staining with anti-α-tubulin antibody (Figure 8B, α-tubulin, lane 2). No binding of α-tubulin to immobilized protein L was detected (Figure 8B, α-tubulin, lane 4).

Probing of the immunoprecipitate with anti-β-tubulin antibody confirmed the presence of β-tubulin subunits (data not shown). Probing of the immunoprecipitate with anti-γ-tubulin antibody (TU-31) revealed that the precipitated αβ-tubulin dimers also contained γ-tubulin (Figure 8B, TU-31, lane 2). Closer inspection of the immunoblots revealed that only the 56-kD protein was coprecipitated. The same band was stained with the anti-γ-tubulin antibody AthTU. When the immobilized antibody was incubated without extract, no staining in the position of γ-tubulin was observed (Figure 8B, TU-31, lane 3). Control antibody VI-10 (IgM) gave no precipitation of γ-tubulin and tubulin dimers (data not shown). Coprecipitation of γ-tubulin with tubulin dimers also was confirmed on extracts prepared from fava bean (Figure 8C). These results strongly suggest that tubulin dimers can interact directly or indirectly with γ-tubulins in plant extracts.

γ-Tubulin Cosedimented with Plant Microtubules Polymerized in Vitro and Was Localized along Their Entire Length

After showing that γ-tubulin interacts with αβ-tubulin dimers, we wanted to elucidate the interaction of γ-tubulin with polymerized microtubules in a spin-down assay we developed previously (Weingartner et al., 2001). Pelleted microtubules, polymerized from Arabidopsis and fava bean extracts, were analyzed for the presence of α-, β-, and γ-tubulin. Because the data for microtubules polymerized from S27 or S100 were similar, only data for S100 are shown. Both of the anti-γ-tubulin antibodies revealed an association of γ-tubulin (56 kD) with polymerized microtubules, as shown for Arabidopsis (Figure 9A, lanes 2 and 3). The 60-kD protein recognized by TU-31 also was associated with microtubules, but compared with γ-tubulin (56 kD), it was not enriched in the microtubular pellet. Control extracts without taxol or DMSO did not provide a tubulin pellet, which excluded a possible nonspecific sedimentation of clustered tubulins (Figure 9A, lanes 4 and 5). The absence of abundant cytoplasmic Ran GTPase in sedimented microtubules (Figure 9A) confirmed the affinity association of γ-tubulin with microtubules.

Because the supernatant S100 contained only a minor part of the large γ-tubulin complexes and no monomeric γ-tubulin (Figure 6), it is likely that soluble smaller γ-tubulin complexes or γ-tubulin oligomers were bound to microtubules. When microtubules were polymerized on slides and, after extensive washing, immunolabeled with anti-γ-tubulin antibodies, both antibodies stained microtubules in a dot-like manner along their entire length (Figure 9B, AthTU and TU-31). The staining pattern was similar to the punctuate staining of γ-tubulin observed along microtubules in cells (Figure 2) (Liu et al., 1993). No such staining was observed when preimmune serum was used as a negative control (Figure 9B, preimmune serum). These results suggest that γ-tubulin or its forms laterally associate with plant microtubules polymerized in vitro.

DISCUSSION

Antibody Tools

The newly prepared polyclonal anti-peptide antibody AthTU against the Arabidopsis γ-tubulin sequence recognizes, on immunoblots of various plant species, a single band in the range 56 to 58 kD. In Arabidopsis, all anti-γ-tubulin antibodies we have used (AthTU, TU-31, and N38-53) stained a 56-kD protein. It is 2 to 3 kD larger than the predicted molecular masses for two Arabidopsis-expressed γ-tubulin genes (53.3 and 53.4 kD), as calculated from their amino acid sequences. γ-Tubulin might run on gels in positions corresponding to relative molecular masses greater than those predicted previously (Ovechkina and Oakley, 2001). Because of this fact, the determination of whether the protein recognized with anti-γ-tubulin antibodies is γ-tubulin or another protein containing the recognized epitope is crucial for further experimental work. Our immunoprecipitation experiments provide direct evidence that the antibodies AthTU and TU-31 recognized the identical 56-kD γ-tubulin protein in Arabidopsis. Moreover, staining of the 56-kD γ-tubulin with AthTU antibody was abolished by preabsorption of the antibody with γ-tubulin peptides used to generate AthTU and/or TU-31 antibodies.

The TU-31 antibody reacted in Arabidopsis extracts not only with the 56-kD protein but also with a 60-kD immunoreactive protein, and corresponding very close bands also were immunodetected in other plant species. The fact that the staining of both protein bands in Arabidopsis was abolished after preabsorption of the TU-31 antibody with each of the two immunizing peptides suggests that the epitope recognized on the SDS-denatured 60-kD protein by TU-31 is similar to or identical with the phylogenetically conserved γ-tubulin amino acid sequence from the C-terminal region of the molecule. A database search showed that no other proteins containing the peptide sequence used to generate the TU-31 antibody or a peptide close to it are found in the Arabidopsis genome. Both the 56-kD γ-tubulin and the 60-kD protein were spun down with microtubules polymerized

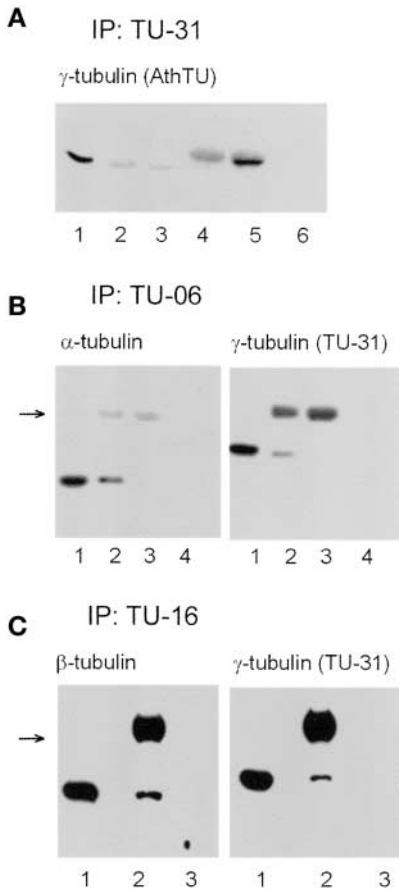

Figure 8. Immunoprecipitation of Cell Extracts with Anti-Tubulin Antibodies.

Proteins were separated by 7.5% SDS-PAGE and immunoblotted. IP, immunoprecipitant.

(A) Immunoblots of Arabidopsis cell extracts precipitated by monoclonal anti-γ-tubulin antibody TU-31 and immunoblotted with polyclonal anti-γ-tubulin antibody AthTU. Lane 1, proteins remaining after precipitation; lane 2, NF-09 antibody (negative control) not incubated with the protein extract; lane 3, immunoprecipitated proteins with NF-09 antibody (negative control); lane 4, TU-31 antibody not incubated with the protein extract; lane 5, immunoprecipitated proteins with TU-31 antibody; lane 6, proteins bound to protein L without antibody.

(B) Immunoblots of Arabidopsis cell extracts precipitated by monoclonal anti-β-tubulin antibody TU-06 and immunoblotted with antibodies TU-01 against α-tubulin and monoclonal antibody TU-31 against γ-tubulin. Lane 1, proteins remaining after precipitation; lane 2, immunoprecipitated proteins; lane 3 immobilized immunoglobulin not incubated with protein extract; lane 4, proteins bound to protein L without antibody. The arrow indicates the position of the IgM heavy chain of the precipitating antibody.

(C) Immunoblots of fava bean extracts precipitated by monoclonal anti-α-tubulin antibody TU-16 and immunoblotted with TUB 2.1 against β-tubulin and anti-γ-tubulin antibody TU-31. Lane 1, proteins remaining after precipitation; lane 2, immunoprecipitated proteins; lane 3, proteins bound to protein L without antibody. The arrow indicates the position of the IgM heavy chain of the precipitating antibody.

from Arabidopsis extracts, and the immunofluorescence staining patterns with TU-31 and AthTU in cells were very similar. Therefore, one cannot exclude completely the possibility that the antibody recognizes two γ-tubulin forms. There are two highly homologous γ-tubulin genes present in the Arabidopsis genome database, but they have identical C-terminal sequences. On the other hand, the 60-kD protein might represent a post-translational modified form of γ-tubulin that has different electrophoretic mobility.

Forms of γ-tubulin differing in their electrophoretic mobility have been distinguished in *Physarum* (Lajoie-Mazenc et al., 1996), *Drosophila* (Raynaud-Messina et al., 2001), brain cells (Sulimenko et al., 2002), and plants (Petitpren et al., 2001). In the latter study, it was found that the 58-kD form was present in all sunflower tissues tested and also was associated with the nucleus, whereas the smaller γ-tubulin (52-kD) form was present only in meristematic and dedifferentiated cells. The subcellular distribution of the 60-kD protein differed from that of the 56-kD γ-tubulin in our experiments as well. Its amount was very limited in the high-speed microsomal fraction; consequently, it was not detected in large γ-tubulin complexes in microsomes. Instead, the 60-kD protein was abundant in the high-speed supernatant in the form of small (120- to 220-kD) complexes or oligomers. The 60-kD protein was not coprecipitated with 56-kD γ-tubulin using AthTU and/or anti-β-tubulin antibody. Therefore, the characteristics of the putative two forms of γ-tubulin (56 and 60 kD) are different. Alternatively, the 60-kD protein represents a protein, sharing the same sequencing epitope as γ-tubulin, that is associated with microtubules. Further protein purification and sequencing is needed for conclusive protein identification.

Heterogeneity of γ-Tubulin Complexes

The presence of γ-tubulin in the form of protein complexes of various sizes in fava bean extracts has been postulated previously (Binarova et al., 2000). Gel filtration analysis, nondenaturing PAGE, and BN-PAGE of the cytosolic fraction from Arabidopsis and fava bean followed by detection with plant-specific antibody revealed the presence of large γ-tubulin complexes (>1 MD) and intermediate-sized complexes. Similar large and intermediate γ-tubulin protein complexes have been reported in different organisms, including fungi (Akashi et al., 1997) and plants (Stoppin-Mellet et al., 2000). The well-characterized large γ-tubulin complexes in animal

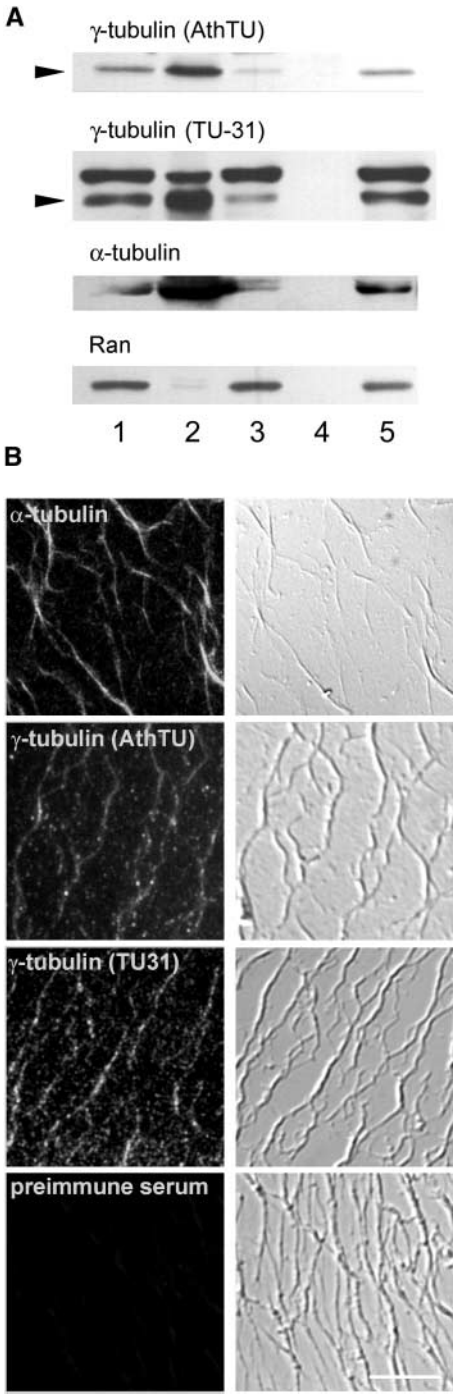

Figure 9. Association of γ-Tubulin with in Vitro–Polymerized Microtubules.

(A) Microtubules were prepared from Arabidopsis extracts (S100) by taxol-driven polymerization and analyzed by immunoblotting with antibodies AthTU and TU-31 against γ-tubulin, DM1A against α-tubulin, and anti-Ran antibody (control). Lane 1, extract; lane 2, microtubule pellet; lane 3, supernatant after taxol polymerization; lanes 4 and 5, as in lanes 2 and 3 but without taxol. Arrowheads indicate the position of the 56-kD γ-tubulin.

(B) Immunofluorescence staining of polymerized microtubules with antibodies AthTU and TU-31 against γ-tubulin, DM1A against α-tubulin, and preimmune serum (control). Slides were observed by fluorescence microscopy (left) and differential interference contrast (right). Bar = 10 μm.

models are γ-TuRCs, with a molecular mass of 2.2 MD (Zheng et al., 1998; Oegema et al., 1999). In contrast to the reported salt sensitivity of γ-TuRC, large γ-tubulin complexes of Arabidopsis and fava bean did not dissociate to smaller complexes in the presence of 500 mM NaCl. Cover slip nucleation assays revealed that only fractions with large complexes affect nucleation activity strongly, whereas salt-sensitive intermediate and smaller complexes basically had no effect on microtubule nucleation. In this respect, large complexes resemble the animal γ-TuRCs, which are the most potent soluble microtubule nucleators (Oegema et al., 1999), whereas variable intermediate-sized plant complexes might present another functional type of tubulin complex.

Association of γ-Tubulin Complexes with Membranes

Solubilization of the microsomal fraction with detergents and BN-PAGE demonstrated that γ-tubulin was associated with membranes in the form of large complexes (>1 MD). Coomassie blue and aminocaproic acid used during BN-PAGE made it possible to estimate the molecular mass of detergent-solubilized, membrane-bound γ-tubulin complexes while avoiding the problem of detergent interference, which appeared during gel filtration of solubilized membrane proteins. Although γ-tubulin itself does not have a consensus membrane binding motif, it is possible that other proteins of the complex mediate its association with membranes. Our data indicate that αβ-tubulin dimers are associated with large membrane-bound γ-tubulin complexes. Interestingly, palmitoylation of the α-tubulin molecule has been described (Caron, 1997). Moreover, an association of γ-tubulin with the protein Tyr kinase p53/p56^{lyn}, whose significant fraction is located in membrane microdomains, has been reported (Draberova et al., 1999b).

Nuclear and cortical membranes are believed to be sites of microtubule nucleation, and studies of both green fluorescent protein–tubulin dynamics (Kumagai et al., 2001) and γ-tubulin immunolocalization (Vaughn and Harper, 1998) support this hypothesis. The plant homolog of Spc98p, a protein that interacts with γ-tubulin in complexes in a broad range of eukaryotes, colocalizes with γ-tubulin on the nuclear envelope in tobacco. Antibodies against Spc98p and

γ-tubulin decreased the ability of isolated nuclei to nucleate purified brain tubulin. However, no direct biochemical evidence for the presence of an Spc98p homolog in plant γ-tubulin complexes was provided (Erhardt et al., 2002). Our results show that large membrane-associated γ-tubulin complexes are active in microtubule nucleation. Also in accordance with biochemical and functional data are our microscopic observations showing that γ-tubulin associated with membranes. The accumulation of γ-tubulin–decorated vesicle-like structures at the spindle anchoring sites on poles in mitosis, in the area of the phragmoplast in cytokinesis, suggests γ-tubulin interaction with membranes. The localization of Golgi membranes in the vicinity of γ-tubulin–decorated spindle poles and results from brefeldin A treatment indicated that correct endomembrane trafficking is a prerequisite for spindle pole organization, and the interaction of γ-tubulin with membranes might be involved directly or indirectly in this process.

In acentriolar early mouse oocytes, γ-tubulin–positive membranous aggregates containing a variety of vesicular structures are suggested to be the centrosomal precursors of a unique ultrastructure (Calarco, 2000). It is possible that similar membrane vesicular structures containing γ-tubulin complexes exist in acentrosomal plant cells. The majority of large γ-tubulin complexes with nucleation activity were present in the high-speed microsomal fraction in which some of the small vesicles were immunogold labeled for γ-tubulin (electron microscopy data not shown). Further characterization of membranous vesicles is in progress. Recently emerging data show that membranous organelles are not organized solely in a passive manner by the cytoskeleton but participate actively in the organization of cytoskeleton structures. It was reported that Golgi-derived vesicles acted as microtubule-nucleating and -organizing sites, with γ-tubulin participating in the process (Chabin-Brion et al., 2001). In plants, evidence for the presence of a signaling molecule (phospholipase D) associated with membranes and microtubules was provided (Gardiner et al., 2001).

Association of γ-Tubulin with αβ-Tubulin Dimers

The colocalization of γ-tubulin along the entire length of plant microtubules with no preference for possible minus ends and its presence with tubulin paracrystals suggested a more complex role of γ-tubulin related to αβ-tubulins than simple microtubule nucleation (Binarova et al., 1998; Panteris et al., 2000). Our present data on the coprecipitation of αβ-tubulin dimer and γ-tubulin confirmed independently an association of soluble γ-tubulin with tubulin dimers in Arabidopsis and fava bean. This finding might reflect the presence of tubulin dimers in γ-tubulin complexes; alternatively, γ-tubulin could be present in cells in some other forms capable of interacting with αβ-tubulin dimers. Tubulin dimers were not found in the majority of animal γ-TuRCs analyzed (Wiese and Zheng, 1999), but variable amounts of tubulin dimers have been reported to coprecipitate with γ-tubulin in preparations from oocytes (Zheng et al., 1995; Lessman and Kim, 2001) and erythrocytes (Linhartova et al., 2002). γ-Tubulin dimers were identified under natural conditions in HeLa cells (Vassilev et al., 1995), and it was shown that γ-tubulin in the brain could form oligomers (Sulimenko et al., 2002).

Our data indicate that a similar situation might exist in plants. Structural models for self-assembly suggest that γ-tubulin should be capable of self-assembling into dimers or protofilament-like oligomers and of interacting laterally with α- or β-tubulin (Inclan and Nogales, 2001). γ-Tubulin was bound to microtubules polymerized from both low-speed and high-speed supernatant (S100). Because monomeric tubulin as well as the large γ-tubulin complexes are almost completely absent in S100, γ-tubulin most likely is bound to microtubules in the form of small complexes or γ-tubulin oligomers. Dot-like γ-tubulin staining of microtubules along their entire length and its accumulation with microtubular bundles suggest a lateral association of γ-tubulin forms. It was shown that γ-tubulin peptides did not interfere with microtubule assembly in vitro and were associated with microtubules along the polymer length (Llanos et al., 1999).

The massive association of γ-tubulin with kinetochore microtubules in cells with regular mitosis, as well as its presence in the vicinity of kinetochores in monopolar mitosis (Binarova et al., 1998), imply a role for γ-tubulin in the organization of the bipolar spindle. Several mutants of *S. pombe* and *A. nidulans* (Hendrickson et al., 2001; Jung et al., 2001) as well as *Caenorhabditis elegans* with γ-tubulin depleted by RNA interference (Strome et al., 2001) showed that in the absence of γ-tubulin, the function of kinetochore microtubules and anaphase chromosome separation were more affected than microtubule nucleation. Moreover, the overlapping roles of γ-tubulin and kinesin in the organization of kinetochore microtubules and in the establishment of spindle bipolarity were proven genetically in *S. pombe* and *A. nidulans* (Paluh et al., 2000; Prigozhina et al., 2001).

Heterogeneity of γ-Tubulin Forms and Microtubule Organization in Plants

The distribution of γ-tubulin protein complexes among various species might underscore the specific need for an organism to regulate its microtubule dynamics and spindle function. In plants, all somatic and gametic cells are acentrosomal; nuclear and cortical membranes are important sites for organizing the microtubular arrays during cell cycle progression. The large γ-tubulin complexes associated with membranes are potent in vitro nucleators of microtubules. Membranes, being dynamic self-organizing systems, can provide flexible microtubule nucleation activity. More generally, an association of γ-tubulin with membranous structures might ensure the nucleation of microtubule arrays not only in plants but also in other eukaryotic cell types with noncen-

trosomal microtubules. The abundance of γ-tubulin in plant cells and the presence of γ-tubulin in protein complexes of various sizes, different properties, and subcellular locations, as well as γ-tubulin interactions with tubulin heterodimers and the association of γ-tubulin complexes or oligomers with microtubules, all could reflect the specific needs of the plant cells. The precise functions of different γ-tubulin forms in the nucleation and organization of plant microtubules remain to be elucidated.

METHODS

Cells

Seedlings of *Arabidopsis thaliana*, fava bean (*Vicia faba*), pea (*Pisum sativum*), and maize (*Zea mays*) were grown, and whole seedlings or root meristems were collected as described previously (Binarova et al., 2000). Cell suspension cultures of Arabidopsis (ecotype Landsberg *erecta*), described by May and Leaver (1993), were obtained from L. Bogre (Royal Holloway University of London). The sample was cultured in 1× Murashige and Skoog (1962) solution (Sigma) and 3% saccharose supplemented with the growth regulators 1-naphthalene acetic acid (2.5 μM) and kinetine (0.25 μM). Cells were cultured with shaking at 24°C with a 16-h photoperiod and 1-week subculture intervals.

Antibodies

γ-Tubulin was detected with the mouse monoclonal antibody TU-31 (IgG2b) (Novakova et al., 1996) prepared against the conserved 16–amino acid peptide EYHAATRPDYISWGTQ corresponding to the human γ-tubulin sequence 434 to 449. To generate rabbit polyclonal antibody AthTU against the 14–amino acid peptide EYKACESPDYIKWG corresponding to the Arabidopsis γ-tubulin sequence 437 to 450, peptide was coupled to keyhole limpet hemocyanin and antibodies were purified on protein A or affinity purified on peptide-coupled Sulfo-Link beads (Pierce). Polyclonal antibody against human γ-tubulin sequence 38 to 53 (EEFATEGTDRKDVFFYN) from the N-terminal region of the molecule was purchased from Sigma. α-Tubulin and β-tubulin were detected using the mouse monoclonal antibodies DM1A and TUB 2.1 (IgG1) (Sigma). For the precipitation of tubulin dimers, mouse monoclonal antibodies TU-06 (IgM) against β-tubulin (Draber et al., 1989) and TU-16 (IgM) against α-tubulin (Draberova and Draber, 1998) were used. As negative controls for immunoprecipitation experiments, the mouse monoclonal antibodies NF-09 (IgG2a) and VI-10 (IgM) against vimentin were used (Draberova et al., 1999a). Polyclonal anti-Ran antibody was obtained from Babco (Richmond, CA), and monoclonal mouse anti-importin antibody and polyclonal rabbit antibody against the *trans*-Golgi network protein TLG were obtained from Affinity BioReagents (Golden, CO) and Secant Chemicals (Winchendon, MA), respectively. Fluorescein isothiocyanate (FITC)– and indocarbocyanate (Cy3)-conjugated anti-mouse and anti-rabbit antibodies were obtained from Jackson ImmunoResearch Laboratories (West Grove, PA). The anti-mouse Ig antibody and anti-rabbit antibody conjugated with horseradish peroxidase were purchased from Amersham Biosciences (Uppsala, Sweden) or from Promega (Madison, WI).

Preparation of Protein Extracts and Solubilization of Membrane Proteins

Root meristems, seedlings, and suspension cells were collected, ground in liquid nitrogen, and thawed in 1 to 2 volumes of extraction buffer (50 mM K-Hepes, pH 7.4, 1 mM $MgCl_2$, 1 mM EGTA, 1 mM EDTA, 100 mM NaCl, 1 mM DTT, and 0.05% [v/v] Nonidet P-40) supplemented with protease [5 μg/mL each of leupeptin, aprotinin, antipain, soybean trypsin inhibitor, and pepstatin and 10 μg/mL 4-(2-aminoethyl)benzenesulfonylfluoride hydrochloride] and phosphatase [1 mM NaF, 0.5 mM Na_3VO_4, and 15 mM β-glycerophosphate] inhibitors. Alternatively, plant material was ground in extraction buffer using a prechilled blender. Crude extracts were centrifuged at 4000*g* for 10 min at 4°C to sediment cell walls, nuclei, and cell debris (P4). Supernatants (S4) were centrifuged subsequently at 27,000*g* for 1 h at 4°C to separate cytosolic fractions (S27) from pellet (P27).

The cytosolic fraction (S27) from Arabidopsis cells and fava bean root meristems was centrifuged further at 100,000*g* for 1 h at 4°C to obtain a high-speed microsomal pellet (P100) and a high-speed supernatant (S100). The pellet (P27) and the microsomal membrane fraction (P100) were resuspended in extraction buffer supplemented with one of the following detergents: 10 mM 3-[(3-cholamidopropyl)dimethylammonio]-1-propanesulfonic acid, 1% β-D-lauryl maltoside, 0.1% Triton X-100, and 0.1% Nonidet P-40. Alternatively, pellets P27 and P100 were treated with 0.1 M Na_2CO_3, pH 11. After 30 min of incubation at 4°C, detergent-insoluble material was centrifuged at 48,000*g* for 20 min at 4°C.

Gel Filtration Chromatography

Gel filtration of cell extracts (fractions S27 or S100) was performed using a fast protein liquid chromatography system with a Superose 12 HR 10/30 column (Amersham Pharmacia). Column equilibration and chromatography were performed in column buffer (50 mM K-Hepes, pH 7.4, 1 mM EGTA, 100 mM NaCl, 2% glycerol, and 1 mM DTT) supplemented with protease and phosphatase inhibitors (see extraction buffer). In some experiments, the column buffer was supplemented with 500 mM NaCl. Fractions (0.25 mL) were collected, and aliquots were used for the preparation of samples for SDS-PAGE or nondenaturing PAGE. The column was calibrated for each particular chromatography condition used. The following molecular mass standards were used: thyroglobulin (669 kD), ferritin (440 kD), catalase (232 kD) (Gel Filtration Calibration Kit; Amersham Pharmacia), alcohol dehydrogenase (150 kD), BSA (66 kD), and ovalbumin (45 kD) (Sigma). Dextran blue (Amersham Pharmacia) was used to determine the column void volume.

Electrophoresis and Immunoblotting

Proteins separated by SDS-PAGE (Laemmli, 1970) were transferred onto nitrocellulose membranes by wet electroblotting. Details of the immunostaining procedure are described elsewhere (Draber et al., 1989). Immunoreactive bands were visualized using either the enhanced chemiluminescence detection system (Pierce) or the alkaline phosphatase detection system (Promega).

In some experiments, anti-γ-tubulin antibodies were preabsorbed with the peptides used for immunization. Both human γ-tubulin peptide (EEFATEGTDRKDVFFYN) and Arabidopsis γ-tubulin peptide (EYKACESPDYIKWG) were used for preabsorption of TU-31 and

AthTU antibody. Peptide corresponding to amino acid residues 38 to 53 of human γ-tubulin was used as a negative control. Two molar ratios of antibody to peptide were used: 1:5 and 1:50. Mixtures of antibodies and peptides were incubated for 30 min at room temperature.

Nondenaturing PAGE was performed using the Laemmli system (Laemmli, 1970), except that SDS was omitted completely and electrophoresis was performed at 4°C. Sample buffer consisted of 62.5 mM Tris-HCl, pH 6.8, 10% glycerol, and 0.01% (w/v) bromphenol blue. Proteins were separated on 3 to 10% linear gradient gels with 3% stacking gels. After electrophoresis, proteins were electroblotted onto nitrocellulose for protein gel blot analysis.

Blue native PAGE (BN-PAGE) was performed using a slightly modified method of Schagger and von Jagow (1991). Microsomal membranes were resuspended in solubilization buffer (50 μM bis-Tris-HCl, pH 7.0, 750 mM aminocaproic acid, and 1% dodecyl-β-D-maltoside). After 20 min of centrifugation at 48,000*g*, the supernatants were supplemented with Coomassie Brilliant Blue G to a final concentration 0.25% and applied to 4 to 15% gradient polyacrylamide gels. In two-dimensional BN-PAGE/SDS-PAGE, strips of lines were cut, soaked in five-times-concentrated SDS sample buffer for 5 min, and mounted on 10% denaturing SDS gels for separation in the second dimension. After electrophoresis, proteins were electroblotted to nitrocellulose. For nondenaturing PAGE and BN-PAGE, the High Molecular Mass Calibration Kit (Amersham Pharmacia) was used.

Immunoprecipitation and Peptide Elution

The supernatant (S27) at a total protein concentration of 3 mg/mL was precleaned using protein A–agarose beads (Pierce) to reduce the nonspecific binding of proteins. Beads saturated with affinity-purified AthTU antibody were washed three times with washing buffer (extraction buffer supplemented with 150 mM NaCl), added to the precleaned extract (50 μL/mL extract), and incubated with rocking for 2 h at 4°C. After washing five times for 10 min with washing buffer, the beads were incubated with immunogenic peptide (1 mg/mL washing buffer) with rocking for 18 h at 4°C to elute γ-tubulin. As a control, immunoglobulins from preimmune serum, or irrelevant antibodies instead of AthTU antibody, were used.

Immunoprecipitation with TU-31 and anti-α-tubulin and anti-β-tubulin antibodies was performed according to Draberova and Draber (1993). Cell extracts (S27) were incubated with beads of protein L (Pierce) saturated with anti-γ-tubulin antibody TU-31, anti-α-tubulin antibody TU-16, anti-β-tubulin antibody TU-06, negative control IgM antibody VI-10, negative control IgG antibody NF-09, or protein L alone. Antibodies were used in the form of 10-times-concentrated spent culture supernatants from hybridoma cells. Sedimented beads (50 μL) with immobilized protein L were incubated with rocking at 4°C for 2 h with 1 mL of corresponding antibody in 0.4 mL of concentrated supernatant (mixed with 0.8 mL of TBST: 10 mM Tris, pH 7.4, 150 mM NaCl, and 0.05% Tween 20). The beads were pelleted, washed four times in TBST, and incubated further with rocking for 3 h at 4°C with 0.5 mL of cell extract diluted 1:1 with TBST. The beads were pelleted and washed four times for 5 min each before boiling for 5 min in 100 μL of SDS sample buffer to release the bound proteins.

Cover Slip Nucleation Assay

A modified cover slip nucleation assay (Oegema et al., 1999) was used to test the microtubule nucleation activity of fractions from gel filtration. Poly-L-Lys–coated cover slips were blocked for 5 min with 1% BSA in blocking buffer (50 mM K-Hepes, 100 mM KCl, 1 mM $MgCl_2$, and 1 mM EGTA, pH 7.6). Blocking solution was replaced with 20 μL of samples (fractions from gel filtration), and after 10 min, the cover slips were washed with buffer BrB80 (80 mM K-Pipes, 1 mM $MgCl_2$, and 1 mM EGTA) supplemented with 10% glycerol and 1 mM GTP. Samples were incubated with 0.5 mg/mL purified bovine brain tubulin (Molecular Probes, Leiden, The Netherlands) in BrB80 buffer. Spontaneous polymerization of purified tubulin on slides without tested samples occurred at tubulin concentrations of 1.5 mg/mL and higher. Therefore, a subcritical tubulin concentration of 0.5 mg/mL was used in all nucleation assays. Cover slips with the samples to be tested attached were incubated for 15 or 60 min; then, the tubulin was removed by aspiration and replaced with 1% glutaraldehyde for 3 min, followed 5 min after fixation by −20°C methanol. The cover slips were rehydrated, and the microtubules were visualized by indirect immunofluorescence with the anti-α-tubulin antibody DM1A.

Microtubule Sedimentation Assay

The microtubule cosedimentation experiments were performed as described previously (Weingartner et al., 2001) with slight modifications. Arabidopsis cells or fava bean root meristems were homogenized in BrB80 buffer and supplemented with protease and phosphatase inhibitors, as described for the extraction buffer. Polymerizations were performed from both the S27 and the high-speed extracts (S100). GTP was added to 1 mM, and taxol was added to 20 μM. Alternatively, DMSO at a final concentration 7.5% was used instead of taxol. After 15 min of polymerization at 37°C, the extracts were loaded onto a 40% Suc cushion in BrB80 buffer and spun down. Microtubules were washed twice by the resuspension of pellets in 10 volumes of BrB80 buffer supplemented with GTP and taxol followed by centrifugation. In control experiments, taxol or DMSO was omitted from the reaction mixture. Washed microtubules were resuspended in SDS sample buffer. For immunofluorescent visualization of in vitro–prepared microtubules, the polymerization mixture was laid on cover slips coated with poly-L-Lys and blocked by BSA, as described for the cover slip nucleation assays. After 15 min of polymerization at room temperature, the excess extracts were removed by aspiration and the cover slips were washed extensively in BrB80 buffer. Samples then were processed for immunofluorescence examination as described for the cover slip nucleation assays.

Immunofluorescence

Root tips or cultured cells were fixed for 1 h in 3.7% paraformaldehyde and processed for immunofluorescence as described previously (Binarova et al., 1993). In some experiments, seedlings were treated with brefeldin A at 200 $\mu g \cdot ml^{-1}$ for 30 min before root tip fixation and immunolabeling. A stock solution of brefeldin A (10 mg/mL) in DMSO was used. Affinity-purified antibody AthTU was used at a dilution 1:100, antibody DM1A was used at a dilution 1:1000, and antibody TU-31 was used as an undiluted supernatant. For double-label immunofluorescence with rabbit and mouse monoclonal antibodies, slides were incubated with the polyclonal antibody, washed, and incubated with the monoclonal antibody. Samples then were incubated simultaneously with a mixture of anti-mouse FITC-conjugated and anti-rabbit Cy3-conjugated secondary antibodies. After 4′,6-diamidino-2-phenylindole staining of DNA and mounting, slides were examined with a confocal laser scanning microscope (TCS/SP;

Leica, Wetzlar, Germany). Laser scanning was performed using the sequential multitrack mode to avoid bleed through. Excitation and emission wavelengths were 488 nm and 505 to 532 nm for FITC and 543 nm and 566 to 600 nm for Cy3. Alternatively, a Provis AX70 optical microscope (Olympus, Tokyo, Japan) equipped with a 100 × 1.4 oil-immersion objective and a Sensi Cam cooled charge-coupled device camera (Kelheim, Germany) coupled with Micro Image Olympus optical software were used. To avoid filter cross-talk, fluorescence was detected using HQ 480/40 exciter and HQ 510/560 emitter filter cubes for FITC and HQ 545/30 exciter and HQ 610/75 emitter filter cubes for Cy3 (both AHF Analysen Technique, Tubingen, Germany). Digital images were processed using Adobe Photoshop 5.5 (Adobe Systems, San Jose, CA).

Upon request, all novel materials described in this article will be made available in a timely manner for noncommercial research purposes.

ACKNOWLEDGMENTS

The authors thank Laczlo Bogre for the gift of the cell suspension of Arabidopsis. This work was supported in part by Grant LN00A081 from the Ministry of Education of the Czech Republic and Wellcome Trust Collaborative Research Initiative Grant 067411/Z/02/Z to P.B., by Grant LN00A026 from the Ministry of Education of the Czech Republic to P.D., and by a postdoctoral grant (204/02/D06S) from the Grant Agency of the Czech Republic to V.C.

Received August 21, 2002; accepted October 29, 2002.

REFERENCES

Akashi, T., Yoon, Y., and Oakley, B.R. (1997). Characterization of gamma-tubulin complexes in *Aspergillus nidulans* and detection of putative gamma-tubulin interacting proteins. Cell Motil. Cytoskeleton **37,** 149–158.

Binarova, P., Cenklova, V., Hause, B., Kubatova, E., Lysak, M., Dolezel, J., Bogre, L., and Draber, P. (2000). Nuclear gamma-tubulin during acentriolar plant mitosis. Plant Cell **12,** 433–442.

Binarova, P., Cihalikova, J., and Dolezel, J. (1993). Localization of MPM-2 recognized phosphoproteins and tubulin during cell cycle progression in synchronized *Vicia faba* root meristem cells. Cell Biol. Int. **17,** 847–856.

Binarova, P., Dolezel, J., Draber, P., Heberle-Bors, E., Strnad, M., and Bogre, L. (1998). Treatment of *Vicia faba* root tip cells with specific inhibitors to cyclin-dependent kinases leads to abnormal spindle formation. Plant J. **16,** 697–707.

Calarco, P.G. (2000). Centrosome precursors in the acentriolar mouse oocyte. Microsc. Res. Tech. **49,** 428–434.

Caliebe, A., Grimm, R., Kaiser, G., Lubeck, J., Soll, J., and Heins, L. (1997). The chloroplastic protein import machinery contains a Rieske-type iron-sulfur cluster and a mononuclear iron-binding protein. EMBO J. **16,** 7342–7350.

Caron, J.M. (1997). Posttranslational modification of tubulin by palmitoylation. I. In vivo and cell-free studies. Mol. Biol. Cell **8,** 621–636.

Chabin-Brion, K., Marceiller, J., Perez, F., Settegrana, C., Drechou, A., Durand, G., and Pous, C. (2001). The Golgi complex is a microtubule-organizing organelle. Mol. Biol. Cell **12,** 2047–2060.

Dibbayawan, T.P., Harper, J.D., and Marc, J. (2001). A gamma-tubulin antibody against a plant peptide sequence localises to cell division-specific microtubule arrays and organelles in plants. Micron **32,** 671–678.

Draber, P., Draberova, E., Linhartova, I., and Viklicky, V. (1989). Differences in the exposure of C- and N-terminal tubulin domains in cytoplasmic microtubules detected with domain-specific monoclonal antibodies. J. Cell Sci. **92,** 519–528.

Draberova, E., and Draber, P. (1993). A microtubule-interacting protein involved in coalignment of vimentin intermediate filaments with microtubules. J. Cell Sci. **106,** 1263–1273.

Draberova, E., and Draber, P. (1998). Novel monoclonal antibodies TU-08 and TU-16 specific for tubulin subunits. Folia Biol. **44,** 35–36.

Draberova, E., Zikova, M., and Draber, P. (1999a). Monoclonal antibody VI-10 specific for vimentin. Folia Biol. **45,** 35–36.

Draberova, L., Draberova, E., Surviladze, Z., and Draber, P. (1999b). Protein tyrosine kinase p53/p56(lyn) forms complexes with gamma-tubulin in rat basophilic leukemia cells. Int. Immunol. **11,** 1829–1839.

Erhardt, M., Stoppin-Mellet, V., Campagne, S., Canaday, J., Mutterer, J., Fabian, T., Sauter, M., Muller, T., Peter, C., Lambert, A.M., and Schmit, A.C. (2002). The plant Spc98p homologue colocalizes with gamma-tubulin at microtubule nucleation sites and is required for microtubule nucleation. J. Cell Sci. **115,** 2423–2431.

Gardiner, J.C., Harper, J.D., Weerakoon, N.D., Collings, D.A., Ritchie, S., Gilroy, S., Cyr, R.J., and Marc, J. (2001). A 90-kD phospholipase D from tobacco binds to microtubules and the plasma membrane. Plant Cell **13,** 2143–2158.

Geissler, S., Pereira, G., Spang, A., Knop, M., Soues, S., Kilmartin, J., and Schiebel, E. (1996). The spindle pole body component Spc98p interacts with the gamma-tubulin-like Tub4p of *Saccharomyces cerevisiae* at the sites of microtubule attachment. EMBO J. **15,** 3899–3911.

Hendrickson, T.W., Yao, J., Bhadury, S., Corbett, A.H., and Joshi, H.C. (2001). Conditional mutations in gamma-tubulin reveal its involvement in chromosome segregation and cytokinesis. Mol. Biol. Cell **12,** 2469–2481.

Inclan, Y.F., and Nogales, E. (2001). Structural models for the self-assembly and microtubule interactions of gamma-, delta- and epsilon-tubulin. J. Cell Sci. **114,** 413–422.

Jung, M.K., Prigozhina, N., Oakley, C.E., Nogales, E., and Oakley, B.R. (2001). Alanine-scanning mutagenesis of Aspergillus gamma-tubulin yields diverse and novel phenotypes. Mol. Biol. Cell **12,** 2119–2136.

Kumagai, F., Yoneda, A., Tomida, T., Sano, T., Nagata, T., and Hasezawa, S. (2001). Fate of nascent microtubules organized at the M/G1 interface, as visualized by synchronized tobacco BY-2 cells stably expressing GFP-tubulin: Time-sequence observations of the reorganization of cortical microtubules in living plant cells. Plant Cell Physiol. **42,** 723–732.

Laemmli, U.K. (1970). Cleavage of structural proteins during the assembly of the head of bacteriophage T4. Nature **227,** 680–685.

Lajoie-Mazenc, I., Detraves, C., Rotaru, V., Gares, M., Tollon, Y., Jean, C., Julian, M., Wright, M., and Raynaud-Messina, B. (1996). A single gamma-tubulin gene and mRNA, but two gamma-tubulin

polypeptides differing by their binding to the spindle pole organizing centres. J. Cell Sci. **109,** 2483–2492.

Lessman, C.A., and Kim, H. (2001). Soluble tubulin complexes in oocytes of the common leopard frog, *Rana pipiens*, contain gamma-tubulin. Mol. Reprod. Dev. **60,** 128–136.

Linhartova, I., Novotna, B., Sulimenko, V., Draberova, E., and Draber, P. (2002). Gamma-tubulin in chicken erythrocytes: Changes in localization during cell differentiation and characterization of cytoplasmic complexes. Dev. Dyn. **223,** 229–240.

Liu, B., Joshi, H.C., Wilson, T.J., Silflow, C.D., Palevitz, B.A., and Snustad, D.P. (1994). γ-Tubulin in Arabidopsis: Gene sequence, immunoblot, and immunofluorescence studies. Plant Cell **6,** 303–314.

Liu, B., Marc, J., Joshi, H.C., and Palevitz, B.A. (1993). A gamma-tubulin-related protein associated with the microtubule arrays of higher plants in a cell cycle-dependent manner. J. Cell Sci. **104,** 1217–1228.

Llanos, R., Chevrier, V., Ronjat, M., Meurer-Grob, P., Martinez, P., Frank, R., Bornens, M., Wade, R.H., Wehland, J., and Job, D. (1999). Tubulin binding sites on gamma-tubulin: Identification and molecular characterization. Biochemistry **38,** 15712–15720.

May, M., and Leaver, C. (1993). Oxidative stimulation of glutathione synthesis in *Arabidopsis thaliana* suspension culture. Plant Physiol. **103,** 621–627.

McDonald, A.R., Liu, B., Joshi, H.C., and Palevitz, B.A. (1993). Gamma-tubulin is associated with a cortical-microtubule-organizing zone in the developing guard cells of *Allium cepa* L. Planta **191,** 357–361.

Moritz, M., Braunfeld, M.B., Sedat, J.W., Alberts, B., and Agard, D.A. (1995). Microtubule nucleation by gamma-tubulin-containing rings in the centrosome. Nature **378,** 638–640.

Murashige, T., and Skoog, F. (1962). A revised medium for rapid growth and bioassays with tobacco tissue culture. Physiol. Plant. **15,** 473–497.

Novakova, M., Draberova, E., Schurmann, W., Czihak, G., Viklicky, V., and Draber, P. (1996). γ-Tubulin redistribution in taxol-treated mitotic cells probed by monoclonal antibodies. Cell Motil. Cytoskeleton **33,** 38–51.

Oegema, K., Wiese, C., Martin, O.C., Milligan, R.A., Iwamatsu, A., Mitchison, T.J., and Zheng, Y. (1999). Characterization of two related Drosophila gamma-tubulin complexes that differ in their ability to nucleate microtubules. J. Cell Biol. **144,** 721–733.

Ovechkina, Y., and Oakley, B.R. (2001). Gamma tubulin in plant cells. Methods Cell Biol. **67,** 195–212.

Paluh, J.L., Nogales, E., Oakley, B.R., McDonald, K., Pidoux, A.L., and Cande, W.Z. (2000). A mutation in gamma-tubulin alters microtubule dynamics and organization and is synthetically lethal with the kinesin-like protein pkl1p. Mol. Biol. Cell **11,** 1225–1239.

Panteris, E., Apostolakos, P., Graf, R., and Galatis, B. (2000). Gamma-tubulin colocalize with microtubule arrays and tubulin paracrystals in dividing vegetative cells of higher plants. Protoplasma **210,** 179–187.

Petitpren, M., Caumont, C., Barthou, H., Wright, M., and Alibert, G. (2001). Two γ-tubulin isoforms are differentially expressed during development in *Helianthus annuus*. Physiol. Plant. **111,** 102–107.

Prigozhina, N.L., Walker, R.A., Oakley, C.E., and Oakley, B.R. (2001). γ-Tubulin and the C-terminal motor domain kinesin-like protein, KLPA, function in the establishment of spindle bipolarity in *Aspergillus nidulans*. Mol. Biol. Cell **12,** 3161–3174.

Raynaud-Messina, B., Debec, A., Tollon, Y., Gares, M., and Wright, M. (2001). Differential properties of the two Drosophila gamma-tubulin isotypes. Eur. J. Cell Biol. **80,** 643–649.

Ritzenthaler, C., Nebenfuhr, A., Movafegi, A., Stussi-Garaud, C., Behnia, L., Staehlin, L.A., and Robinson, D.G. (2002). Reevaluation of the effect of brefeldin A on plant cells using tobacco Bright Yellow 2 cells expressing Golgi-targeted green fluorescent protein and COPI antisera. Plant Cell **14,** 237–261.

Schagger, H., and von Jagow, G. (1991). Blue native electrophoresis for isolation of membrane protein complexes in enzymatically active form. Anal. Biochem. **199,** 223–231.

Stoppin-Mellet, V., Peter, C., and Lambert, A.M. (2000). Distribution of γ-tubulin in higher plant cells: Cytosolic γ-tubulin is a part of high molecular weight complexes. Plant Biol. **2,** 290–296.

Strome, S., Powers, J., Dunn, M., Reese, K., Malone, C.J., White, J., Seydoux, G., and Saxton, W. (2001). Spindle dynamics and the role of gamma-tubulin in early *Caenorhabditis elegans* embryos. Mol. Biol. Cell **12,** 1751–1764.

Sulimenko, V., Sulimenko, T., Poznanovic, S., Nechiporuk-Zloy, V., Bohm, K., Macurek, L., Unger, E., and Draber, P. (2002). Association of brain tubulin with alpha/beta-tubulin dimers. Biochem. J. **365,** 889–895.

Vassilev, A., Kimble, M., Silflow, C.D., LaVoie, M., and Kuriyama, R. (1995). Identification of intrinsic dimer and overexpressed monomeric forms of gamma-tubulin in Sf9 cells infected with baculovirus containing the Chlamydomonas gamma-tubulin sequence. J. Cell Sci. **108,** 1083–1092.

Vaughn, K.C., and Harper, J.D. (1998). Microtubule-organizing centers and nucleating sites in land plants. Int. Rev. Cytol. **181,** 75–149.

Vorobjev, I.A., Svitkina, T.M., and Borisy, G.G. (1997). Cytoplasmic assembly of microtubules in cultured cells. J. Cell Sci. **110,** 2635–2645.

Weingartner, M., Binarova, P., Drykova, D., Schweighofer, A., David, J.P., Heberle-Bors, E., Doonan, J., and Bogre, L. (2001). Dynamic recruitment of Cdc2 to specific microtubule structures during mitosis. Plant Cell **13,** 1929–1943.

Wiese, C., and Zheng, Y. (1999). Gamma-tubulin complexes and their interaction with microtubule-organizing centers. Curr. Opin. Struct. Biol. **9,** 250–259.

Wiese, C., and Zheng, Y. (2000). A new function for the gamma-tubulin ring complex as a microtubule minus-end cap. Nat. Cell Biol **2,** 358–364.

Zheng, Y., Wong, M.L., Alberts, B., and Mitchison, T. (1995). Nucleation of microtubule assembly by a gamma-tubulin-containing ring complex. Nature **378,** 578–583.

Zheng, Y., Wong, M.L., Alberts, B., and Mitchison, T. (1998). Purification and assay of gamma tubulin ring complex. Methods Enzymol. **298,** 218–228.